Piles for Stabilising Seismically Precarious Slopes. Part B : Parametric Analysis and Design Charts

R. Kourkoulis, F.Gelagoti, I. Anastasopoulos, G. Gazetas
Soil Mechanics Laboratory, National Technical University Athens, Greece

ABSTRACT: The simplified numerical model formulated and validated in the companion paper is utilized to perform parametric analyses of piles embedded in an unstable slope undergoing lateral soil movement. Pile diameter and spacing, depth of pile embedment, soil layering and stiffness are the key problem parameters investigated. Dimensionless Charts are developed for guiding the design of piles for slope stabilization.

1. INTRODUCTION

The pile design methodology presented in the companion paper involves two steps: (a) perform a simple slope stability analysis to obtain the force required to stabilize the slope and (b) use of design charts providing the maximum shear force that may be offered by the piles in order to decide upon the optimum pile configuration. The present paper deals with the second step, aiming at exploring the effect of key problem parameters on the behavior of slope stabilizing piles.

2. PARAMETRIC ANALYSES

Both cohesive and non-cohesive soils have been utilized to model the "unstable" soil. The interface depth from the surface (H_u), is varied parametrically, covering from a shallow (H_u = 4m) to a very deep (H_u = 12 m) landslide.

A plethora of parametric analyses have been performed for the behaviour of slope stabilizing piles nailing unstable soil layers of various depths and material properties. The factors examined are:

(a) Effect of Pile Spacing
(b) Inhomogeneity of the Unstable Soil
(c) Strength of the Stable Soil Layer
(d) Depth of Pile Embedment into the Stable Layer
(e) Pile Non-linearity

2.1. *Soil Arching between the Piles*

Wang and Yen (1974) studied analytically the behavior of piles in a rigid-plastic infinite soil slope with emphasis on arching effects, and concluded that a critical pile spacing exists in both sandy and clayey slopes, beyond which practically no arching develops. In general, arching stems from the stress transfer through the mobilization of shear strength. It is the transfer of stress from "yielding" parts of a soil mass to adjoining non-yielding or less compliant parts.

Two cases of pile arrangement are compared: a dense pile spacing assumed to ensure arching and a loose one where the piles are distant and soil can freely flow between them. It is assumed that loading is imposed on the free field (i.e. far enough from the pile region) on the soil nodes. It is supposed that after application of the load, the pile displacement has a value of u_p, while the soil between the piles displaces u_{ip}. Soil arching is measured with the ratio u_{ip}/u_p . If this ratio ranges between 1 and at most 2, the pile and neighboring soil displace almost equally and the piles are effective thanks to arching. For much higher u_{ip}/u_p ratios arching is not effective.

As an example Fig.1 displays two characteristic snapshots of the FE analyses. The unstable soil layer is considered to be a sand with $\varphi = 28^o$, $\psi = 2^o$, and $c = 3$ kPa. The bottom soil layer is assumed to be very hard soil (bordering on soft rock) with $S_u = 600$ kPa. The interface properties are $\varphi = 16^o$, $c = 3$ kPa, and $\psi = 1^o$ Its location is assumed at 4m depth from the ground surface. The top figure plots the displacements contours on the ground surface for the case of piles of diameter $D = 1.2$m spaced center-to-center at 2D, i.e, 2.4 m. From the distribution of displacement contours distribution it is evident that the soil between the piles has been restricted by the presence of the piles hence displaced almost equally with them—a clear manifestation of arching. On the contrary, in the case of piles spaced at 7D (bottom figure), the intermediate soil has not been confined by the piles and flows between them.

3D numerical parametric analyses have been performed to define the maximum pile spacing that ensures sufficient degree of arching as a function of their diameter. The results are summarized in Fig. 2, which plots the dependence of the U_{ip} / U_p ratio on U_p/U_p^{max}. It is apparent that spacings of 2, 3 and 4 times the pile diameter are able to provide soil arching. For spacings greater than 5 diameters soil flows between the piles; such arrangements are therefore not applicable to slope stabilization and will not further examined. Evidently, the most effective pile arrangement in terms of arching is the spacing of 4 diameters. However, the 2D and 3D cases of will be examined since the piles "attract" smaller forces in these cases.

2.2. *Effect of Pile Spacing*

Spacings of 2, 3 and 4 times the pile diameter have been investigated. While, increasing pile spacing improves their effectiveness, it nevertheless reduces the total resistance force offered per unit width. The total stiffness and capacity of the soil-pile system is a function of both pile spacing and height of the unstable soil layer. In the case of the shallow landslide of H_u = 4m (Fig. 3), RF is nearly independent of pile spacing. In the deep landslide (H_u = 8m), (Fig. 4), the differences among the different pile spacings are clear : since the soil-pile system is much more flexible, hence requiring a substantially increased pile deformation for the same Resistance Force (RF). Note that these results refer to elastic piles of diameter D = 1.2m. In case of the non-linear pile, the maximum realistic moment that may be developed must not exceed the actual structural strength of the pile. Hence, it must be pointed out that although the maximum value of RF developed (elastically) is nearly independent of pile spacing for all landslide depths, the only acceptable ultimate RF values are those which are achieved at acceptable levels of the bending moment.

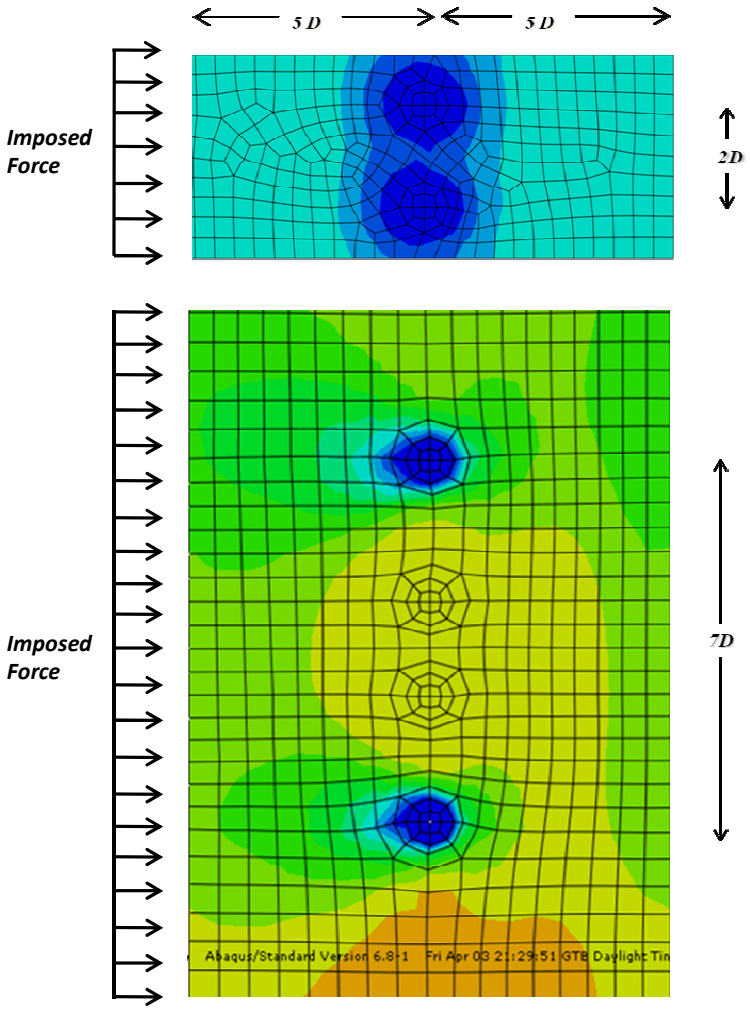

Figure 1. Contours of horizontal displacements (a) of a dense pile configuration (distance between piles 2D) and (b) of a sparse pile configuration (pile distance 7D).

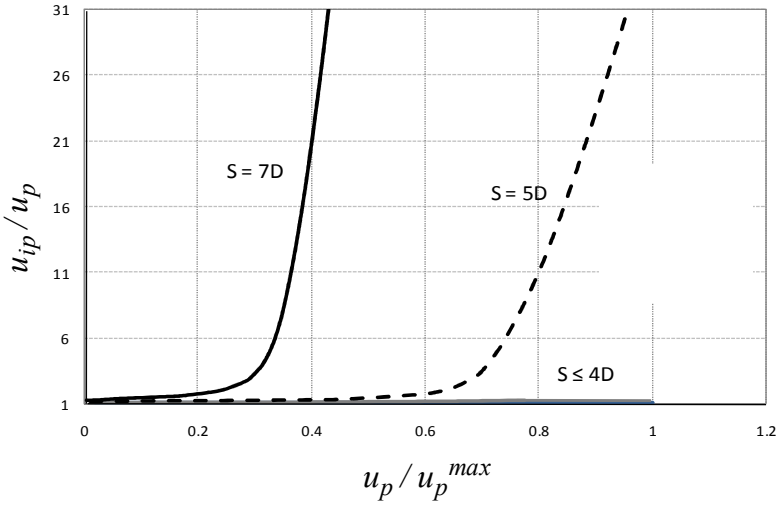

Figure 2. Comparison of the interpile displacements calculated for different pile spacings in sandy soil. It is obvious that for spacings $S > 5D$, soil flows between the piles.

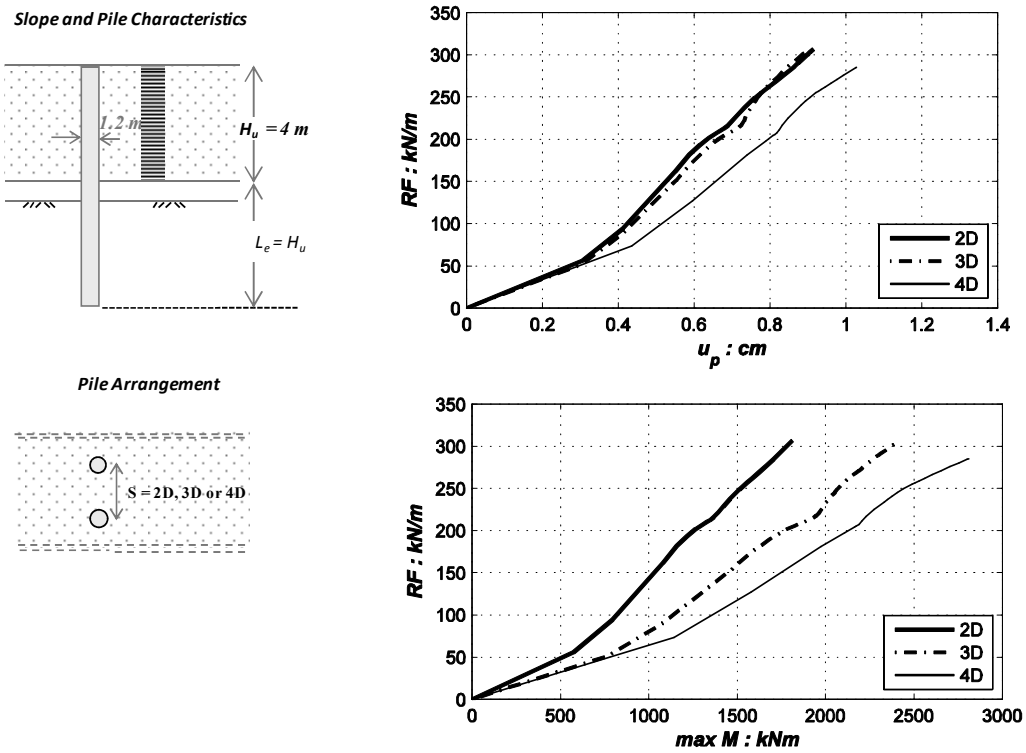

Figure 3. Resistance Force (*RF*) offered by the pile vs Pile head displacement diagrams and *RF* vs maximum Bending Moment Diagrams for various pile spacings in case of a shallow landslide of H_u = 4m

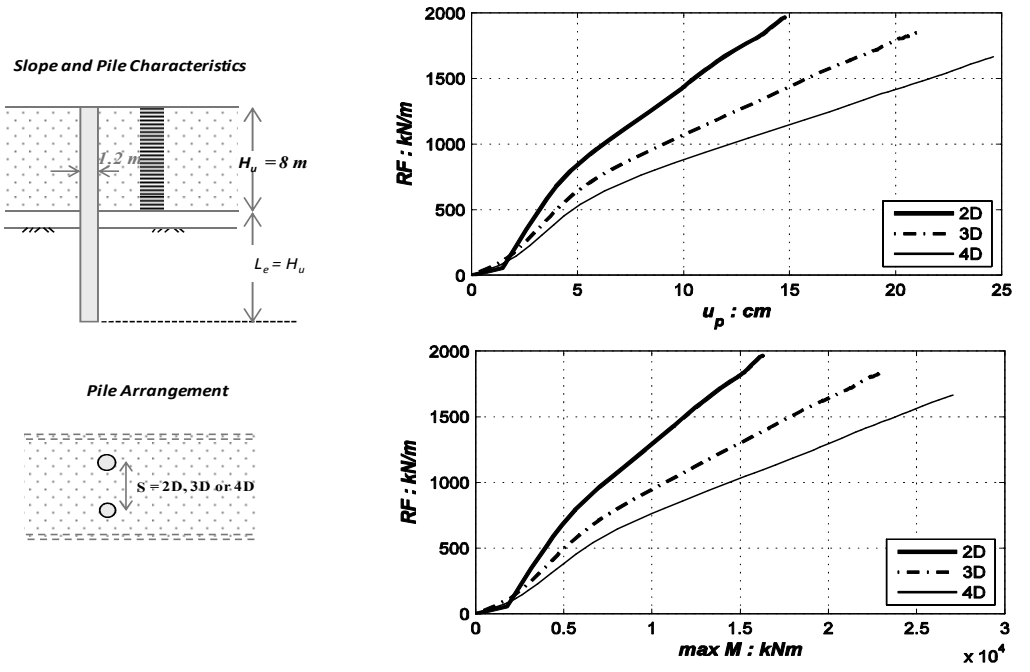

Figure 4. Resistance Force offered by the pile vs Pile head displacement diagrams and *RF* vs maximum Bending Moment Diagrams for various pile spacings in case of a deep landslide of H_u = 8m.

2.3. Effect of Soil Inhomogeneity

Both homogeneous and non-homogeneous soils in terms of elasticity modulus have been investigated. For the case of non-homogeneous soils the modulus has been assumed to vary linearly but with the same mean value as the homogeneous soil. For the cases examined, soil inhomogeneity only faintly affects the results in the shallow landslide case of H_u = 4 m which involves very small displacements.

2.4. Effect of Pile Non-linearity

Both linear and non-linear piles have been examined. For the case of non-linear piles, the considered longitudinal reinforcement is the maximum amount allowed by the Greek Reinforced Concrete Code (EKOS 2000) : 4% of the cross-sectional area. Pile non-linearity is introduced via its Moment Curvature relationship. The ultimate Moment value for the case of a pile diameter of D = 1.2 m is M_{ult} = 7.2 MNm.

Discrepancies between the linear and non-linear pile are noticed only in flexible soil-pile systems, i.e. either in sparsely spaced piles or with deep landslide. In the shallow landslide case (H_u = 4m), the system behaviour is practically elastic; hence the difference in the behaviour between the two pile types is negligible (Fig. 5). On the contrary, the differences are conspicuous in the deep landslide case (Fig. 6). The behaviour of the two types is the same as long as the pile remains below its yielding point. Once the ultimate bending moment is reached, RF offered by the non-linear pile does not increase further. However, up to that point the two pile types behave identically.

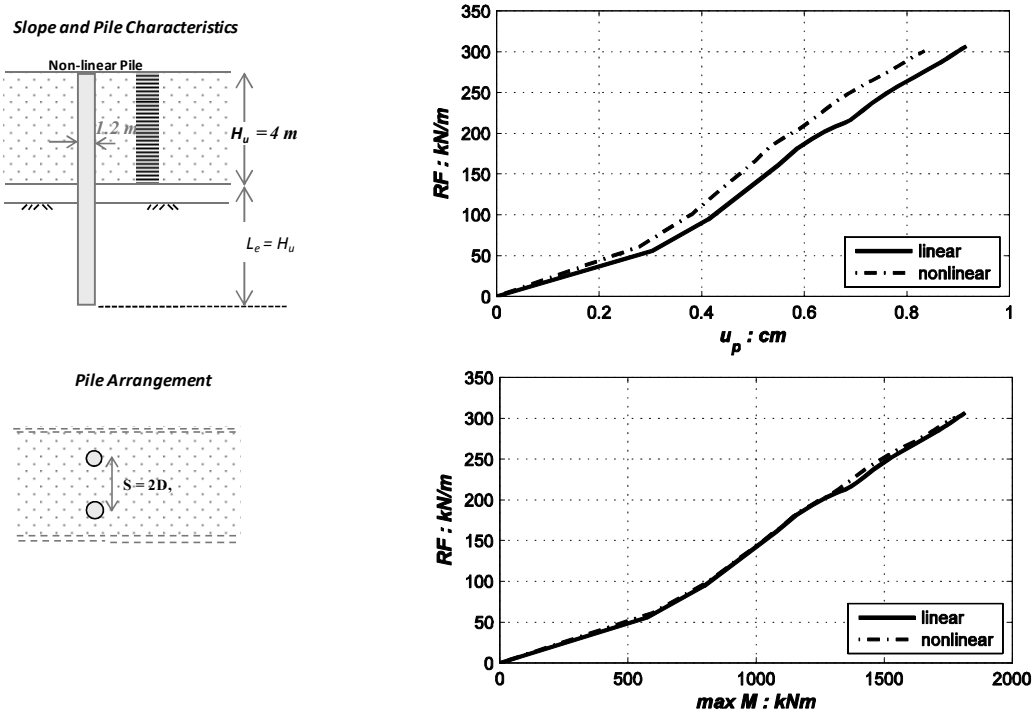

Figure 5. *RF* vs Pile head displacement diagrams and *RF* vs maximum Bending Moment Diagrams with and without considering pile non-linearity in case of a shallow landslide of H_u = 4m

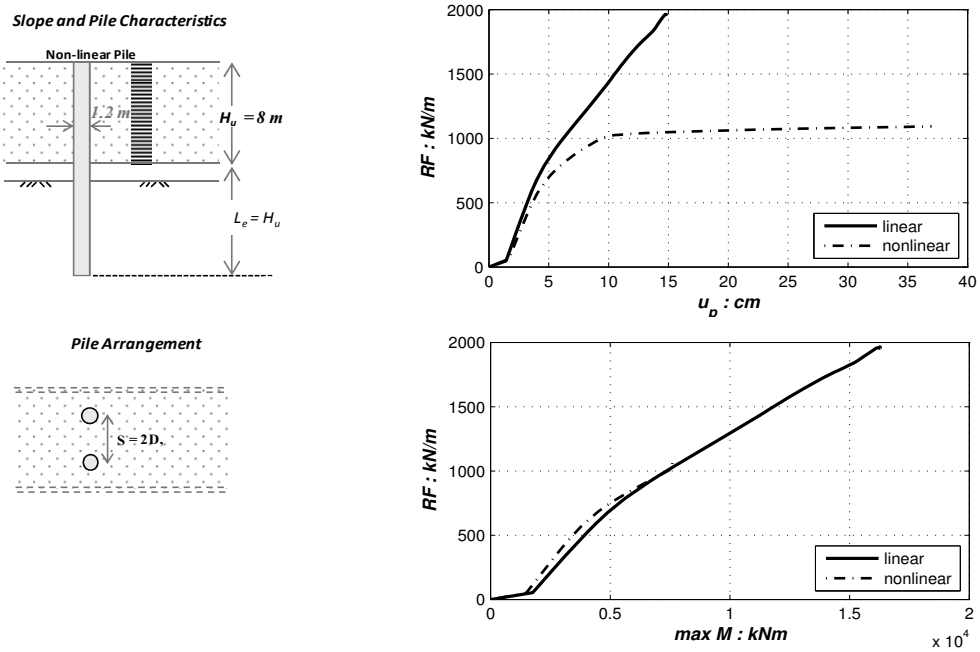

Figure 6. RF vs Pile head displacement diagrams and RF vs maximum Bending Moment Diagrams with and without considering pile non-linearity in case of a deep landslide of H_u = 8m

2.5. Effect of the Strength of the Underlying Stable Ground

The strength and stiffness of the stable soil varied parametrically to model materials ranging from a relatively soft sand of low strength to a very stiff rock. The soils examined are:

(a) *loose silty sand* : $\varphi = 28^o, \psi = 2^o,\ \ c = 3\ kPa\ , G\ =\ 16\ MPa$
(b) *dense sand* : $\varphi = 38^o,\ \psi = 2^o\ , c = 0\ kPa\ , G\ =\ 32\ MPa$
(c) *soft rock* : $\varphi = 45^o, \psi = 5^o\ , c = 50\ kPa\ , G = 1.2\ GPa$
(d) *stiff rock* : $\varphi = 45^o, \psi = 5^o\ , c = 100\ kPa\ , G = 4\ GPa$

The strength parameters of the *stable layer* have been chosen so that the ultimate lateral pile soil pressure be compatible with the ultimate passive soil pressure of the *unstable* layer. The latter is defined as $(P_u)_{unst} = a\ K_p\ \sigma'_{vo}$ for cohesionless soils, as $(P_u)_{unst} = N_p S_u$ for clayey soils of undrained shear strength Su (Broms 1964)

The strength properties of each stable soil type examined correspond to the following values of the ultimate lateral pile soil pressure P_u.

i. $P_{u_s} = (P_u)_{unst}$ for the *loose sand*

ii. $P_{u_s} = 1.6(P_u)_{unst}$ for the *dense sand*

iii. $P_{u_s} = 3(P_u)_{unst}$ for the *soft rock*

iv. $P_{u_s} = 6(P_u)_{unst}$ for the *rock*

The stable layer strength determines the fixity conditions of the pile below the interface. As expected, the analysis reveals that the very soft stable layer is unable to provide adequate fixity

conditions, thus enabling the rotation of the pile as a rigid body. Conversely, with a stiff stable layer, the pile displacement is mainly attributed to its deformation and thus leads in development of substantial bending moments. Fig. 7 reveals that a pile embedded in the low strength substratum would not provide the same level of ultimate resistance as when embedded in a stiff stratum, unless it is greatly displaced.

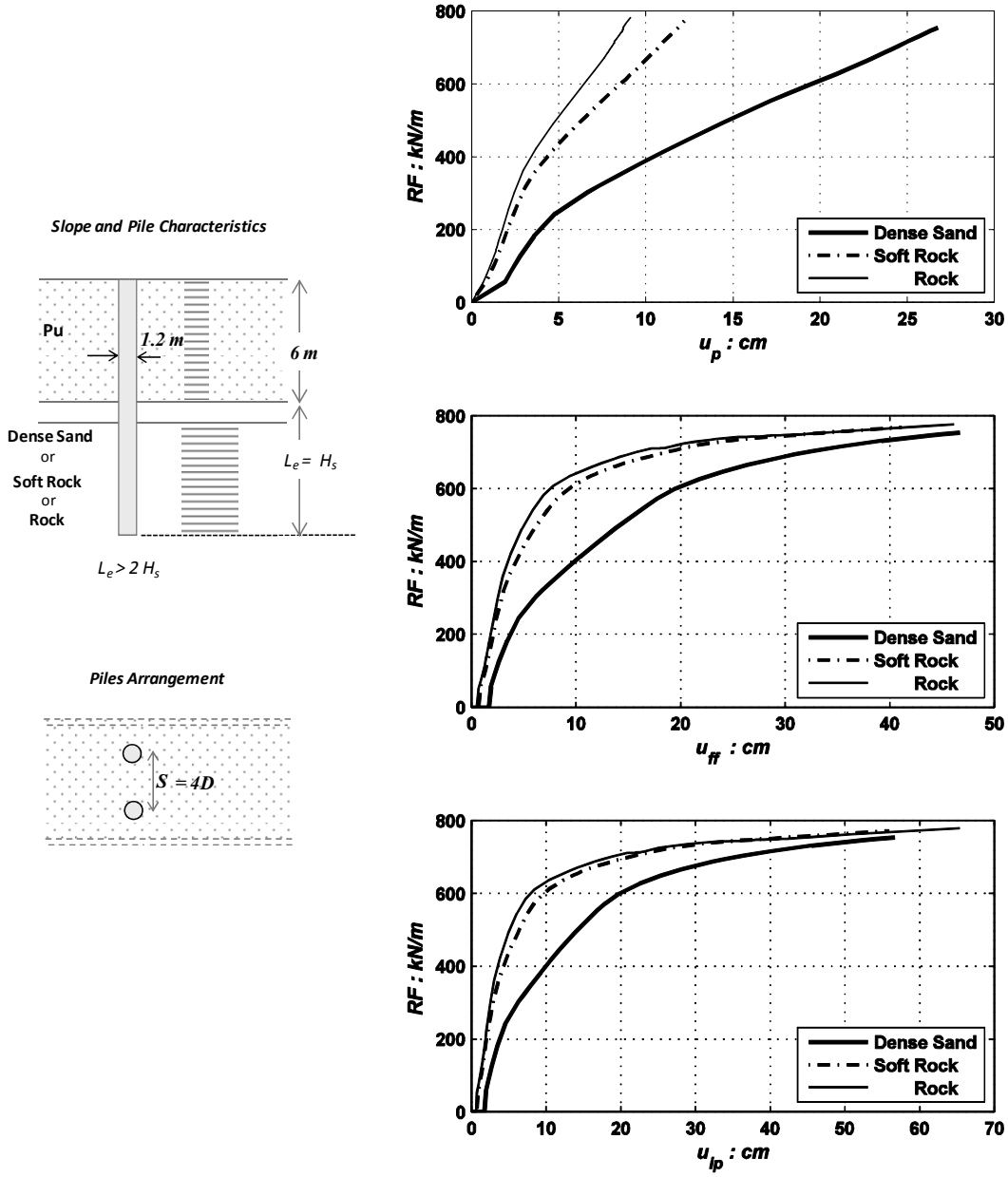

Figure 7 (a). The *effect of the stiffness of the Stable* Ground.Unstable Ground Characteristics: *G=16 MPa, φ=28^o, c=1 kPa, H_u= 6m*. Pile Characteristics: *D=1.2m, L_e=H_S, , S = 4D,* Elastic pile.

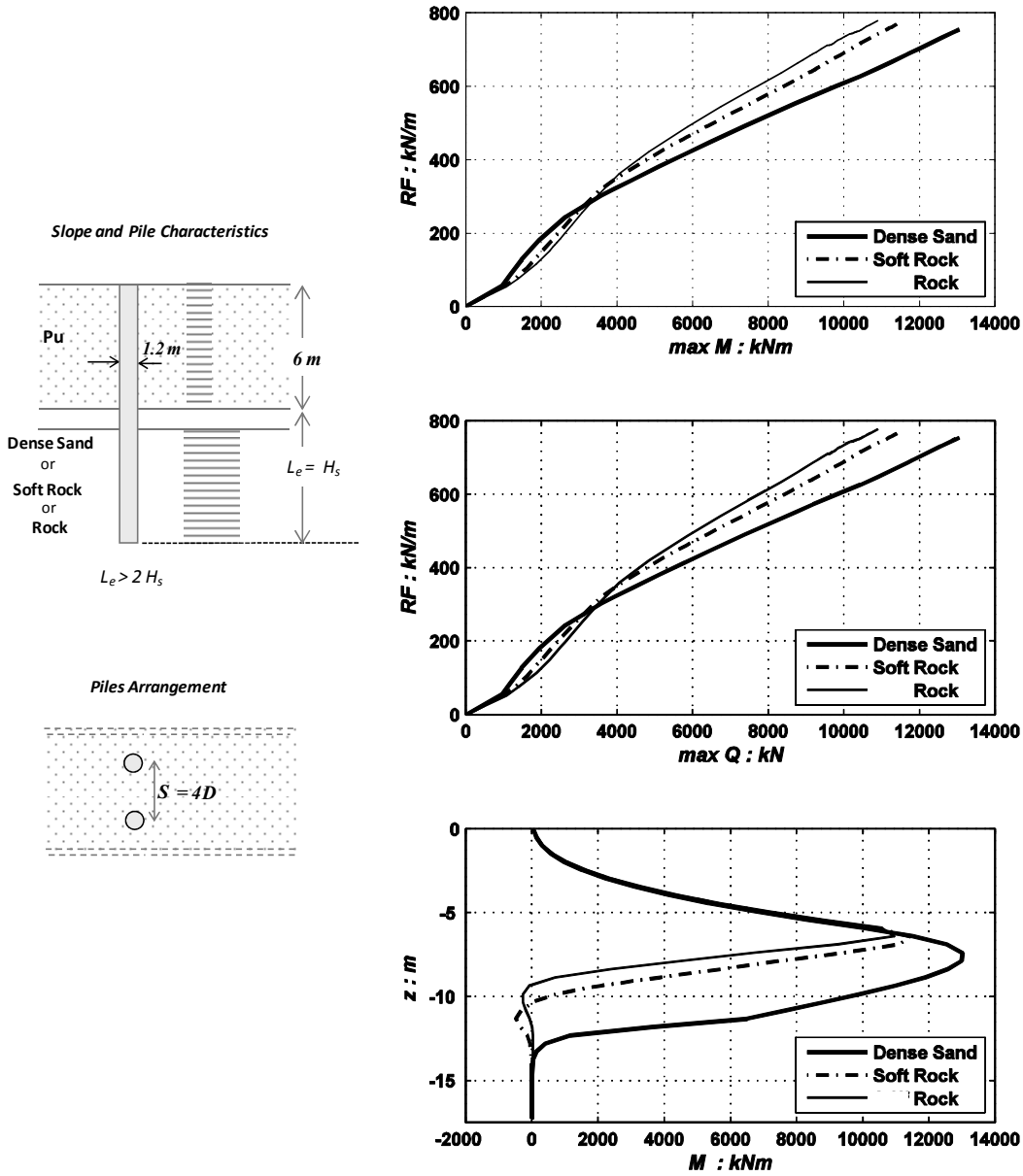

Figure 7(b). *Effect of the stiffness of the Stable* Ground.Unstable Ground Characteristics: *G=16 MPa, φ=28^o, c=1 kPa, H_u= 6m*. Pile Characteristics: *D=1.2m, L_e=H_S, S=4D,* Elastic pile. *(συνέχεια)*

2.6. *Effect of the Depth of Pile Embedment (L_e)*

The depth of the embedment of the pile into the stable ground influences the pile behavior, depending on the strength of the soil and the thickness of the sliding soil that must be stabilized. The embedment depth L_e is expressed as a function of the height H_u of the unstable block. The values examined are: $L_e = 0.7\ H_u$, H_u, 1.2 H_w, and 1.5 H_u

From the results (Fig.8 and Fig. 9) it appears that the required embedment increases with decreasing stable soil strength. Insufficient embedment depth results in rigid body-type rotation of the pile (Fig. 10). The optimum pile embedment depth will be this which ensures adequate pile fixity while remaining economical.

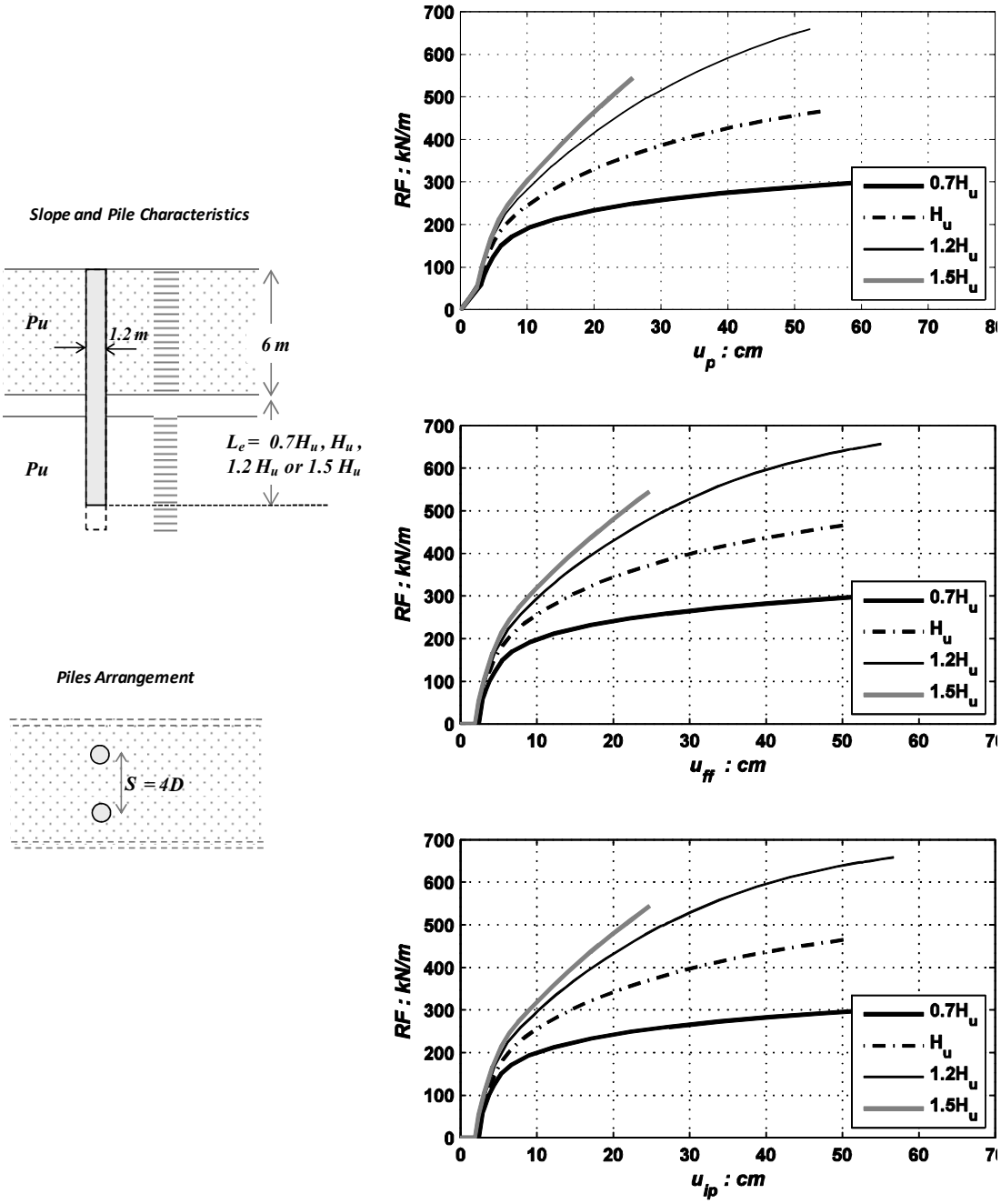

Figure 8. *Effect of Pile Embedment Length*. Unstable Ground Characteristics: *E=40 MPa, φ=28^o, c=1 kPa, H_u= 6m*. Stable Ground Characteristics: *E=40 MPa, φ=28^o, c=1 kPa.* Pile Characteristics: *D=1.2m, S=4D,* Elastic pile.

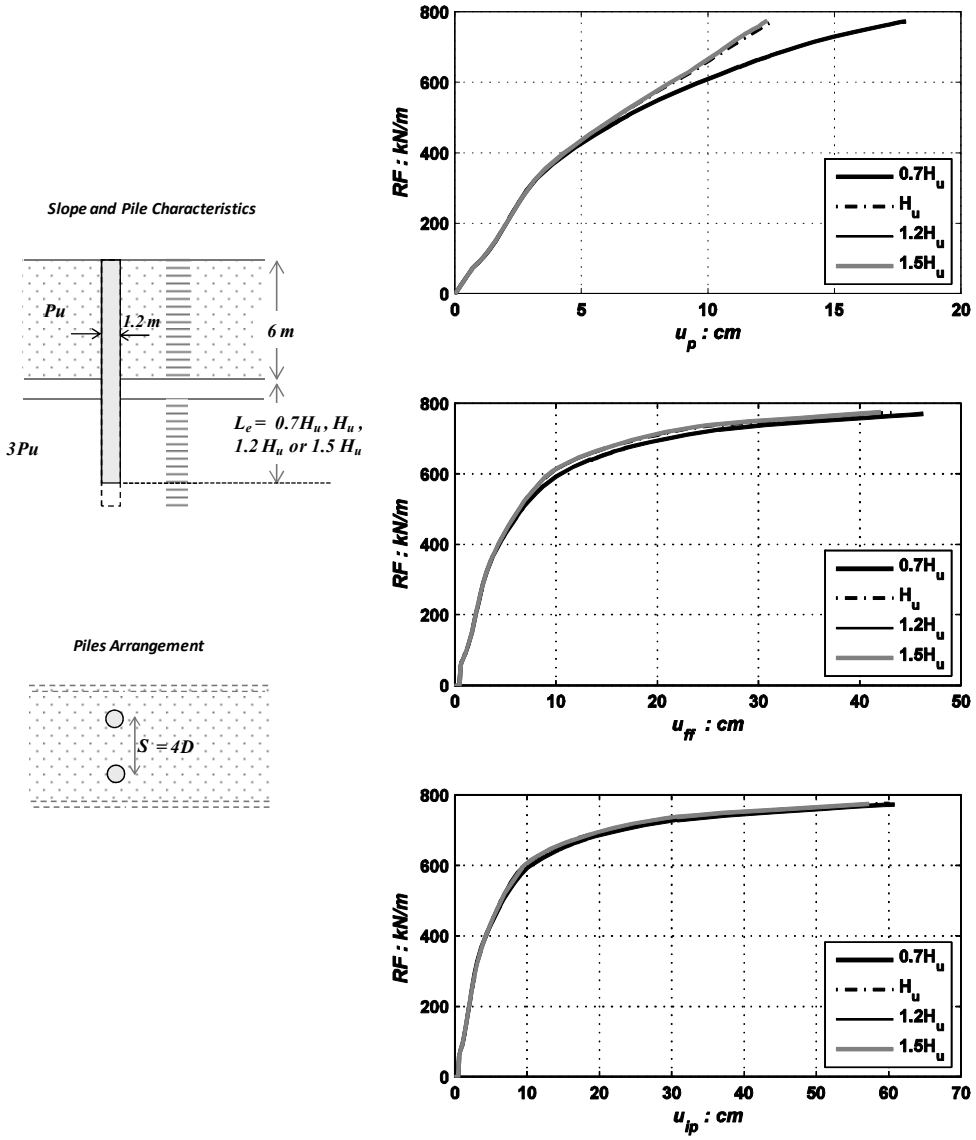

Figure 9. Parametric Analysis Results investigating the *effect of Pile Embedment Length*. Unstable Ground Rock with Characteristics: *G=16 MPa, φ=28°, c=1 kPa, H_u= 6m*. Stable Ground Characteristics: *E=3 GPa, φ=42°, c=50 kPa.* Pile Characteristics: *D=1.2m, S=4D,* Elastic pile.

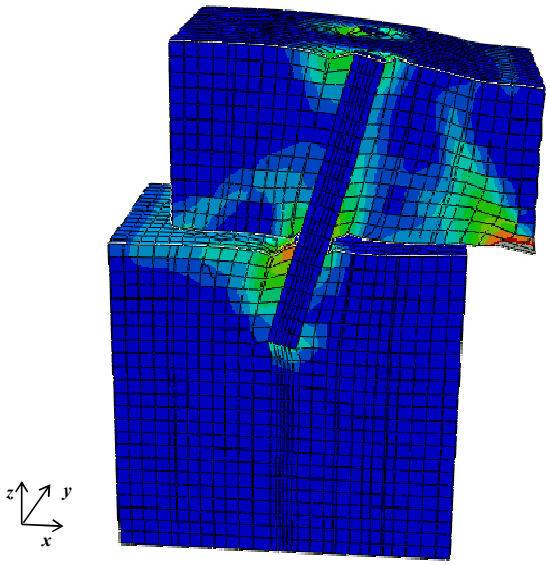

Figure 10. Snapshot of the FE analysis of pile subjected to lateral soil movement. The insufficient embedment depth of the pile leads to its rigid-body-type rotation.

3. PRODUCTION OF DESIGN CHARTS FOR SINGLE PILES

Design charts have produced with non-linear finite elements analyses utilizing the versatile Numerical Model presented and validated in the companion paper by *Kourkoulis et al (2009)*. Fig. 11 is one such set of charts.

Each graph in this figure portrays

a. Resistance Force per unit width (RF) vs Imposed Displacement at Free Field (u_{ff}).

This plot actually provides the ultimate lateral resistance offered by the pile. The plateau of RF defines the maximum calculated Resistance Force (RF) per unit width that may be offered by the specific pile configuration. However, RF should always be considered in conjunction with the required displacement.

b. Resistance Force per unit width (RF) vs Pile Head Displacement (u_p)

c. Reaction Force per unit width (RF) vs Soil Displacement between Piles (u_{ip})

The aim of this plot is clearly the investigation of the effect of arching. Although it has already been discussed in the previous section that all the configurations and spacings examined provide adequate arching, soil displacement between the piles (although small enough as to not signify failure) is not independent of pile spacing. Therefore for reasons similar to those described above, it is considered necessary that the soil displacement information should be available to the designer.

d. Reaction Force per width (RF) vs Pile maximum Bending Moment (maxM)

and

e. Reaction Force per unit width (RF) vs Pile maximum Shear Force (maxQ)

f. Distribution of Bending Moment M vs depth z at the moment of failure

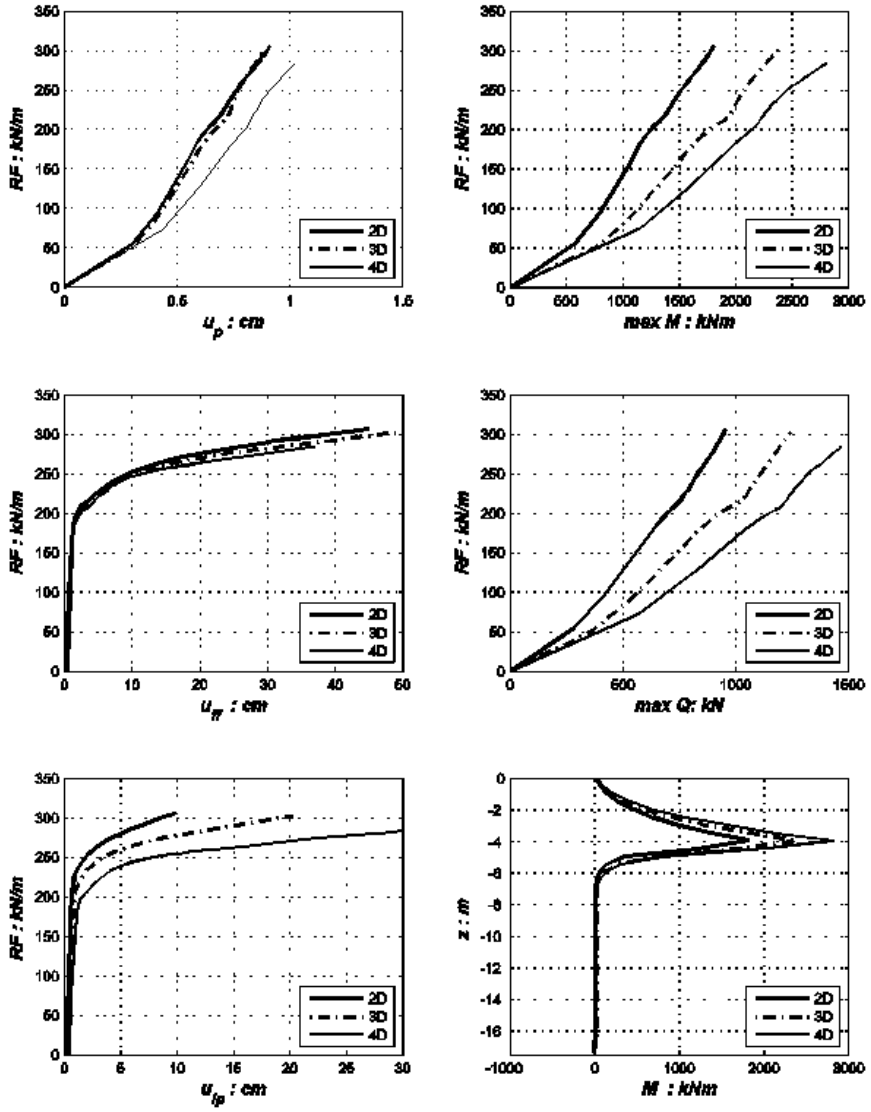

Figure 11. Example design chart

4. DIMENSIONAL ANALYSIS

It is understandable, that design charts such as these above cannot cover all possible soil profiles and pile dimensions. Therefore, a dimensional analysis has been attempted, refering to concrete piles embedded only in very stiff soil, and considering only the "flow mode" type of failure. *This mode creates the least damaging effect of the soil movement on the pile. Poulos (1999) suggests that efforts should be made to promote this mode of behavior.* The embedment length is assumed to be equal to the unstable soil layer depth thus providing adequate fixity conditions.

According to Π-theorem (Langhaar 1951; Barenblatt 1996), the terms involved in the calculation of the pile ultimate load may be combined to form 3 independent dimensionless variables. For the case of non-cohesive soil, this study adopts the following correlation among independent variables:

$$\frac{u_p\, H_u^3}{10^3 D^4} = f\left(\frac{RF}{3\, K_p\, D\, \gamma\, H_u^2},\ \frac{S}{D},\ \frac{H_u}{D}\right) \tag{1}$$

The first term in this equation $u_p H_u^3/10^3 D^4$ will be refered to as *dimensionless pile displacement.* The term D^4 / H_u^3 may be considered as an index of the pile rigidity (assuming fixity at the interface). Increasing the pile rigidity reduces pile displacements. The term $RF/3\ K_p\ D\ \gamma\ H_u^2$ represents the *dimensionless soil-pile system ultimate resistance*.

The term S/D apparently represents the piles distance as a function of the pile diameter. As S/D increases, the dimensionless ultimate resistance term increases, i.e group interaction effects are less pronounced enhancing the efficiency of each pile, as the pile spacing increases.

The term H_u/D is defined as the pile *slenderness ratio* and depends on the height of the soil mass contained between the piles. As the ratio increases, the same amount of RF will be achieved at a higher displacement.

Two dimensionless Charts in Figures 12(a) and 12(b) materialize Eq.(1) for ***soil-pile system ultimate resistance*** as a function of the ***dimensionless displacement*** for cohesionless soils. The curves are plotted for two slenderness ratios:

- $H_u/D = 3.2$ representing a rigid soil-pile system and
- $H_u/D = 5$ which represents a flexible soil-pile system.

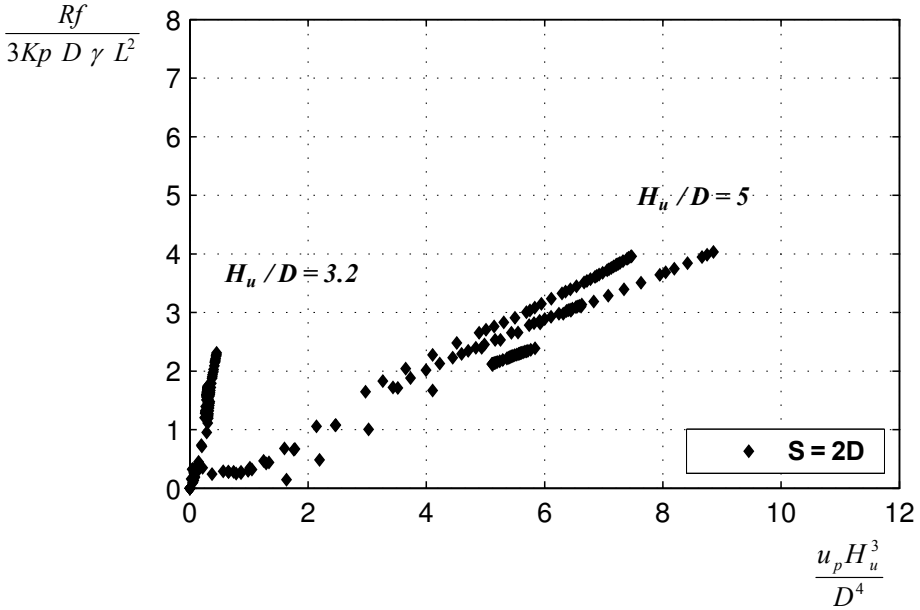

Figure 12 (a). Results of Dimensional Analysis for the case of single piles spaced at 2D embedded in *sandy* soil (pile fixity is assumed just below the interface).

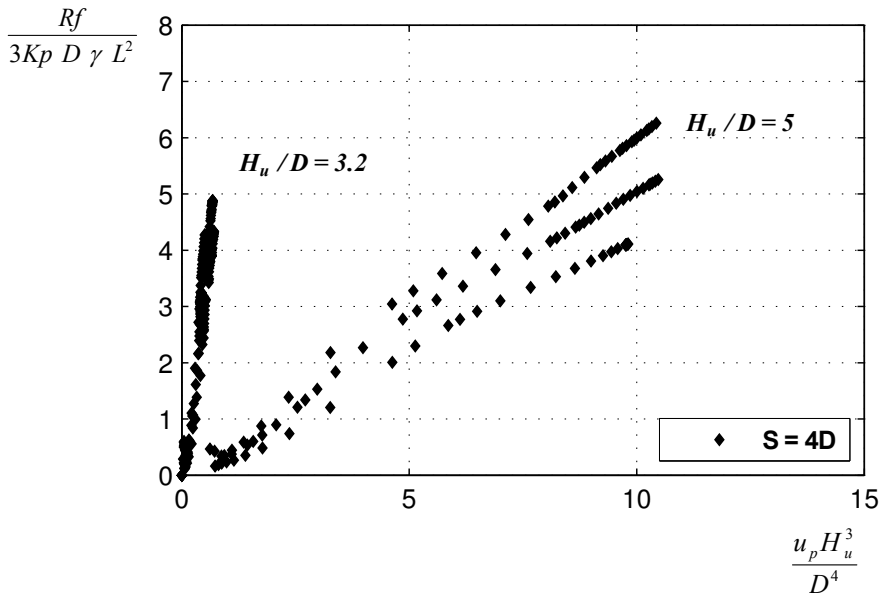

Figure 12b. Results of Dimensional Analysis for the case of single piles spaced at 4D embedded in sandy soil (pile fixity is assumed just below the interface).

ACKNOWLEDGEMENT

The research presented in this paper was financially supported by the Secretariat for Research and Technology of Greece, under the auspices of PENED Programme with Contract number 03ED278.

REFERENCES

Barenblatt, G. I.(1996). "Scaling, self-similarity, and intermediate asymptotics", *Cambridge University Press*, Cambridge, U.K.

Broms, B., (1964), "Lateral resistance of piles in cohesionless soils", *J. Soil Mech. Foundations Div. ASCE*, 90, pp. 123-156

EKOS, (2000), Greek *Reinforced Concrete Code*, Ministry of Public Works, Athens, Greece

Kourkoulis, R., Gelagoti, F., Anastasopoulos, I., Gazetas, G., (2009), "An improved method for the design of Slope Stabilising Piles – Part A: Development and Validation", *Proc. 3rd Greece – Japan Workshop on Seismic Design, Observation and Retrofit of Foundations*, Santorini.

Langhaar, H. L. (1951). "Dimensional analysis and theory of models",*Wiley*, New York.

Poulos H.G. (1999) "Design of slope stabilizing Piles", *Slope Stability Engrg*, Yagi, Yamagami and Jiang, Balkema, Rotterdam

Wang WL, Yen BC., (1974), "Soil arching in slopes", *Journal of the Geotechnical Engineering Division*, ASCE;100(No. GT1), pp. 61–78.